Multimedia Tools and Applications
https://doi.org/10.1007/s11042-018-6535-y

Interstitial lung disease classification using improved DenseNet

Wenping Guo [1,2] · Zhuoming Xu [1] · Haibo Zhang [2]

Received: 31 May 2018 / Revised: 8 August 2018 / Accepted: 10 August 2018
Published online: 15 August 2018

Abstract
Interstitial Lung Disease (ILD) is one of the popular respiratory diseases. The correct diagnosis of ILD is beneficial to improve the effect of treatment for patients. This paper presents an improved DenseNet called small kernel DenseNet (SK-DenseNet) to improve ILD classification performance. According to the characteristics of HRCT features of lung disease, the SK-DenseNet network is more effective to extract high level and small pathological features for ILD classification. Our experiment results show that the proposed SK-DenseNet obtains an outstanding performance (~98.4%),which improves 5% performance compared with DenseNet. A comparative analysis with other CNNs, such as AlexNet, VGGNet, ResNet has also demonstrated that the effectiveness of SK-DenseNet in terms of classifying lung disease patterns is superior than those compared ones. The research has validated that using small convolution kernel is useful to improve the recognition efficiency when feature patterns are small.

Keywords Interstitial lung disease · Deep learning · Convolutional neural network · DenseNet · SK-DenseNet

1 Introduction

The term Interstitial Lung Disease (ILD) was first proposed at the 18th Aspen Lung Conference in 1975 [6], which often refers to a group of more than 200 chronic lung

✉ Wenping Guo
gwp@hhu.edu.cn

Zhuoming Xu
zmxu@hhu.edu.cn

Haibo Zhang
zhanghb@tzc.edu.cn

[1] College of Computer and Information, Hohai University, Nanjing 210098, China

[2] Institute of Intelligent Information Processing, Taizhou University, Taizhou 317000, China

disorders characterized by inflammation of the lung tissue [2]. The most common symptoms of an ILD are shortness of breath, dry cough, labored breathing which cause a serious negative effect for people's daily life. In 2013, ILD affected 595,000 people globally and resulted in 475,000 deaths [1, 25]. Usually a physician will be able to diagnose ILD using a chest X-ray or lung CT scan or pulmonary function testing, even open lung biopsy. Presently, the patterns of ILD is diagnosed by a radiologist using different features of HRCT (High-Resolution Computed Tomography) of lung images. Effectively diagnosing a huge number of HRCT images is currently a very challenging task for even experienced physicians because they need not only to overcome fatigues caused by repetitive work, but also have to concentrate on distinguishing very similar clinical manifestations from the samples. It is important to help ILD classification with machine learning methods to reduce pathological specialists' burden and improve work efficiency, which will improve the effect of treatment for ILD patients.

With remarkable advances in technology, HRCT scanning has played a more and more important role to diagnose ILD [18]. The emergence of large-scale dataset of ILDs, like multimedia database of ILDs from the University Hospital of Geneva [8] accelerated the ILDs detection related research [3, 5, 15, 21]. Accurate classification of ILD patterns could help clinician make better decisions. However, the quite different tissue patterns could result in the same patterns of ILD (See Fig. 1), due to the different physical conditions of patients. Therefore, effectively classifying ILD patterns still represents a challenge to radiologists, respiratory specialists and computer scientists.

In this paper, we focus on classification of five main patterns of ILDs — *healthy tissue, emphysema, ground glass, fibrosis,* and *micronodules*. The rest of the paper is organized as follows. Related work is given in Section 2. In Section 3, we describe SK-DenseNet for ILD classification. The experiments and evaluations are discussed in Section 4. Finally, we conclude our research in Section 5.

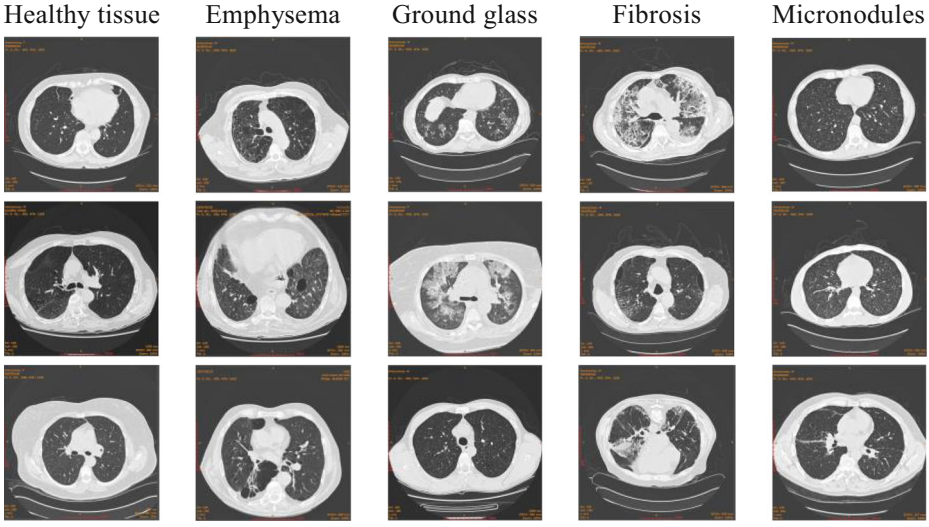

Fig. 1 Three example of each tissue category

2 Related work

Over the last decade, many researches have been conducted on ILD classification. The research interests of ILD classification have been focusing on analyzing texture of HRCT images because the differences between ILD patterns are mainly manifested in image texture. There are two major methods for texture feature selection: hand-crafted features and learned features.

Hand-crafted features are often used the first order gray statistics, gray level co-occurrence matrix, run length matrix and so on, to extract the texture feature of HRCT images [7, 31]. Then use machine learning methods, such as Support Vector Machine (SVM) [9], Random Forest [4], Bayes classifier [24], K Nearest Neighbor (KNN) [23], Linear Discriminant Classifier [17], Sparse Representation [22] and other classification methods for ILD classification.

However, hand-crafted features are characterized by insufficient reliability, which often fail to apply to new data and patterns. The emergence of deep learning has inspired a new solution to this problem.

Deep learning was introduced by Hinton et al. in 2006 [13] which have made great success in many fields, including speech recognition [14, 32], image processing [26–28], person re-identification [29, 30], facial expression recognition [33, 34], and so on. In 2015, Song et al. [22] use Restricted Boltzmann Machine (RBM) to generate multi-scale features automatically, and then use the learned features to convolution with ILD CT images for generating feature vectors. This feature vector can automatically adjust according to the original data. Therefore, this method has a good performance to be adapted to new data and patterns. Although RBM can generate image features automatically, it is still necessary to design the classifier manually. It is challenging to choose appropriate classifiers to divide the extracted feature space. In 2016, Anthimopoulos et al. [5] proposed an improved model for CT image classification based on LeNet Convolution Neural Network. Using the end-to-end advantages of deep neural networks, the training model can determine image features and classifier at the same time, and achieve better classification performance. In 2017, Huang et al. [16] pointed out that the LeNet Convolution Neural Network does not make full use of the features of the previous layers of the neural network. On the basis of this, Huang et al. presented a new DenseNet (Dense Convolutional Network) in order to utilize the training features.

However, the size of input image of DenseNet is 224×224, while the size of the ILD HRCT patch is 32×32. In addition, the feature size in patch is small. In 2015, Simonyan et al. designed a ConvNet [20] using three 3×3 convolution layers instead of a single 7×7 layer, which won the first place in the localization for ImageNet Challenge 2014. The result shows that the small kernel can improve the performance for ConvNet. Therefore, we propose an improved DenseNet called small kernel DenseNet (SK-DenseNet) for ILD classification according to the characteristics of small HRCT image features.

3 Methods

In this section, we firstly describe the problem description and motivation, then introduced the original DenseNet. Our proposed small kernel DenseNet (SK-DenseNet) is introduced in details at last.

3.1 Problem description

Interstitial Lung Disease (ILD) comprises more than 200 lung defects affecting patients' ability to breathe. ILDs are proved to be the textural alterations in the lung parenchyma. Gao et al. [10] divides ILD classification problem into two levels: slice-level classification and patch-level classification (Regions of Interest provided by [8]).

In this study, we focus on patch-level classification for five main patterns of ILDs —*healthy tissue, emphysema, ground glass, fibrosis, micronodules*. So, the problem is to classify each image patch P into one of the five patterns of ILDs, which denoted the five patterns as P_h, P_e, P_g, P_f, P_m. The objective of the problem is to minimize the error of classification.

3.2 Motivation

In order to improve architecture of a Convolutional Neural Network for the classification of ILD patterns, we consider the nature of the problem. ILD patterns in HRCT images usually characterized by the small local textural features. The size of input image of DenseNet is 224 × 224, while the size of the ILD HRCT patch is 32 × 32. In addition, Simonyan et al. [20] shows that the small kernel can improve the performance for ConvNet. Therefore, we propose an improved DenseNet called small kernel DenseNet (SK-DenseNet) for ILD classification according to the characteristics of small HRCT image features.

3.3 DenseNet

The DenseNet architecture [16] is first proposed on CVPR conference in 2017, consisting of several dense blocks. Each layer in dense block has the same feature-map size. Figure 2

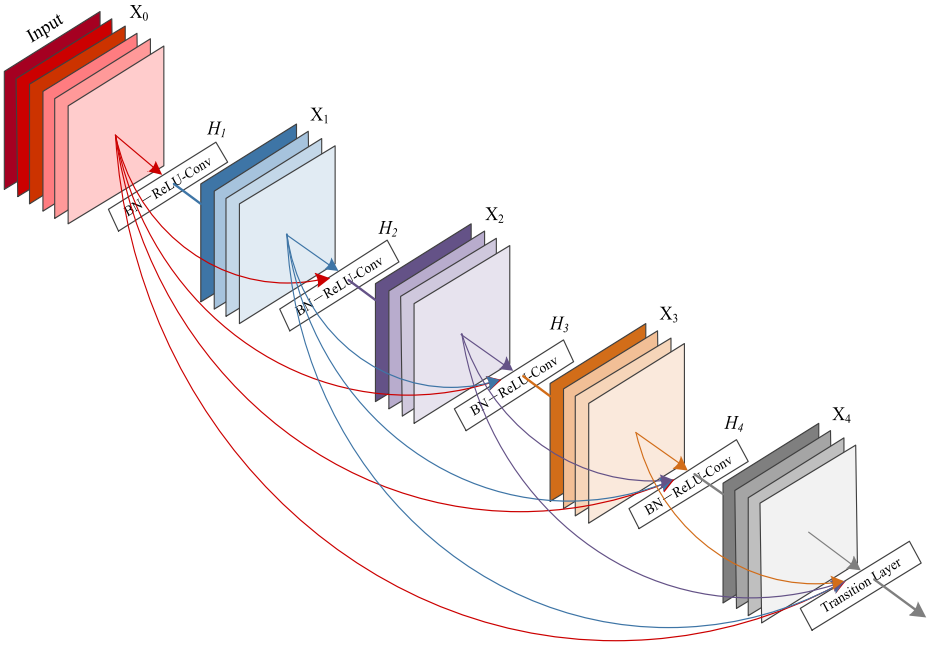

Fig. 2 Architecture of DenseNet

illustrates the architecture of original DenseNet, where the t^{th} layer receives all the preceding layers, x_0, ...,x_{t-1} as the input, see Eq. (1):

$$x_t = H_t([x_0, x_1, \cdots, x_{t-1}]) \tag{1}$$

where $[x_0, ...,x_{t-1}]$ refers to the concatenation of the feature-map produced in layers *0, ..., t-1*. H_t represents the serial process of layer t with Batch Normalization (BN), ReLU, convolution (Conv).

3.4 Proposed SK-DenseNet

In order to improve classification performance, we proposed a small kernel DenseNet (called SK-DenseNet) for ILD classification.

(1) Architecture

Figure 3 describes the architecture of our proposed SK-DenseNet, which contains 2 dense blocks and 2 transition layers. Each dense block contains 6 groups, which are denoted as group 1 to group 6 on the bottom half of Fig. 3. The structures from group 1 to group 6 are the same, which constain a 1 × 1 bottleneck layer and is followed by two 2 × 2 CNN layers.

(2) Activations

In this study, we use *softmax* function on the last layer and Rectified linear units (ReLU) function on the rest layers. *Softmax* function is a generalization of the logistic function that can be used to represent a categorical distribution. Equation (2) gives the formula of the *softmax*:

$$\mathrm{p}(y = j|x_i) = \frac{e^{x_i^T w_j}}{\sum_{k=1}^{K} e^{x_i^T w_k}} \tag{2}$$

for $j = 1, 2, 3, ..., K$,K is the number of samples.

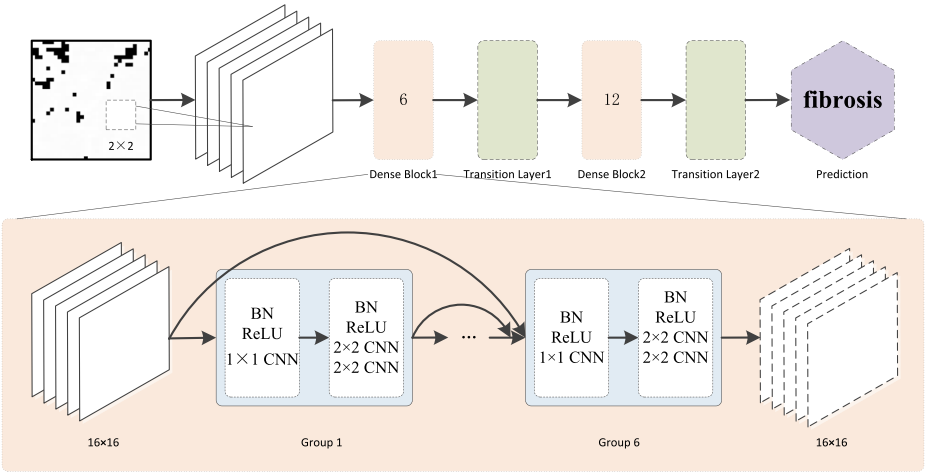

Fig. 3 Architecture of our proposed SK-DenseNet

ReLU function $f(x) = \max(0, x)$ is a most popular activation function which was first introduced to a dynamical network in a paper in Nature [11]. ReLU function, compared to sigmoid function or similar activation function, has several advantages: (1) Better gradient propagation (2) Efficient computation (3) Biological plausibility.

(3) Loss function

In this study, we use the cross entropy to represent the dissimilarity of the predicted output distribution from the true distribution of labels. The formula of cross entropy is Eq. (3):

$$L(x, y) = -\sum_{x} y_i \log\left(f\left(x_i^T w_i\right)\right) \tag{3}$$

where x denotes the set of sample,$y_i$is true distribution for i^{th} sample,$f\left(x_i^T w_i\right)$ is prediction distribution for i^{th} sample.

(4) Optimizers

There are several optimizers which can be used to minimize the loss function, such as Stochastic Gradient Descent (SGD), Adaptive Gradient algorithm (AdaGrad), and Adaptive Moment Estimation (Adam).

To minimize the objective function, SGD would perform the following iterations (See Eq. (4)), AdaGrad would perform the following iterations (See Eq. (5)) and Adam would perform the following iterations (See Eq. (6)):

$$w_{t+1} = w_t - \frac{\eta}{N} \sum_{i=1}^{N} \nabla L\left(x_i^T w_t\right) \tag{4}$$

where N denotes the number of samples in one batch.

$$\begin{aligned} G_{ii} &= \sum_{\tau=1}^{t} g_{\tau i}^2 \\ w_{t+1} &= w_t - \frac{\eta}{\sqrt{G_{ii}}} g_t \end{aligned} \tag{5}$$

where $g_{\tau i}$ denotes the i^{th} element of the $g_\tau g_\tau$denotes the gradient, at iteration τ.

$$\begin{aligned} m_{t+1} &= \beta_1 m_t + (1-\beta_1) g_t \\ v_{t+1} &= \beta_2 v_t + (1-\beta_2) g_t^2 \\ \hat{m} &= \frac{m_{t+1}}{1-(\beta_1)^{t+1}} \\ \hat{v} &= \frac{v_{t+1}}{1-(\beta_2)^{t+1}} \\ w_{t+1} &= w_t - \frac{\eta \times \hat{m}}{\sqrt{\hat{v}} + \varepsilon} \end{aligned} \tag{6}$$

where ε is a small scalar used to prevent division by 0, and β_1 and β_2 are the forgetting factors for gradients and second moments of gradients.

Our experiment results (See Table 3) show that Adam has better performance, which improve 8.2 and 2.4% respectively compared to SGD and AdaGrad.

Table 1 Patient numbers for each lung disease

Disease Classes	Patient Numbers
Healthy tissue	14
Emphysema	9
Ground glass	31
Fibrosis	32
Micronodules	15

4 Experiments and evaluations

4.1 Dataset

The dataset used in experiments is the publicly available multimedia database of ILDs from the University Hospital of Geneva [8], which has 109 HRCT of different ILDs with resolution 512×512 per slice. The dataset consists of 2062 ROI of lung HRCT, which manual annotated by 3 experienced radiologists for 17 different ILD patterns. The popular research patterns contain 5 classes with 931 ROIs of 89 patients, namely *healthy tissue, emphysema, ground glass, fibrosis, micronodules*. The number of patients and ROI are given in Tables 1 and 2 respectively.

4.2 Evaluations

To evaluate the performance of the proposed method we use a train-validation-test scheme. The training set was used for the actual training of the method, while fine turning the hyper-parameters was carried out on the validation set. The performance of all approaches was assessed on the test set. Due to its insensitive to imbalances in the classes, we used the average F-score over the different classes (See Eq. (7)).

$$F_{avg} = \frac{1}{5}\sum_{x=1}^{5} 2 \times \left(\frac{\text{recall}_x \times \text{precision}_x}{\text{recall}_x + \text{precision}_x}\right) \tag{7}$$

where

$$\text{recall}_x = \frac{\text{samples correctly classified as x}}{\text{samples of class x}}$$

$$\text{precision}_x = \frac{\text{samples correctly classified as x}}{\text{samples of classified as x}}$$

Table 2 ROI numbers for each lung disease

Disease Classes	ROI Numbers
Healthy tissue	157
Emphysema	92
Ground glass	209
Fibrosis	260
Micronodules	213

Table 3 Testing results for different hyper-parameters

Pooling type	Kernel size	Number of Dense block	Activation function	Optimizer	Testing result (F_{avg})
ave	2 × 2	[6,12,24,16]	Relu	Adam	0.966
ave	2 × 2	[6,12,24]	Relu	Adam	0.976
ave	2 × 2	[6]	Relu	Adam	0.970
ave	3 × 3	[6,12,24,16]	Relu	Adam	0.933
ave	3 × 3	[6,12,24]	Relu	Adam	0.954
ave	3 × 3	[6,12]	Relu	Adam	0.956
ave	3 × 3	[6]	Relu	Adam	0.948
max	2 × 2	[6,12]	Relu	Adam	0.968
max	2 × 2	[6]	Relu	Adam	0.964
ave	2 × 2	[6,12]	tang	Adam	0.974
ave	2 × 2	[6]	tang	Adam	0.965
ave	2 × 2	[6,12]	Relu	SGD	0.902
ave	2 × 2	[6,12]	Relu	AdaGrad	0.960
ave	2 × 2	[6,12]	Relu	Adam	0.984

4.3 Experiments and discussions

The proposed method was implemented using *Tensorflow* framework and coded in Python programming language. All experiments were performed under a Linux OS on a *HP Z840* workstation with *CPU Intel Xeon E5–2690 v3*2 @ 2.6GHZ, GPU NVIDIA Quadro M6000 24GB*, and *512GB* of *RAM*.

(1) Tuning of hyper-parameters

Hyper-parameters in CNN consist of learning rate, number of convolution layers, kernel size, pooling type, number of neurons in the hidden layer, loss function, activation function, etc. The choice of hyper-parameters can affect the learning rate and the performance of classification.

Table 3 provides testing results for different hyper-parameters of the network. The proposed settings, presented on the bottom in bold, yield the best result F_{avg} of *0.984*. Using 4 dense blocks with the same configurations as the proposed method, would reduces the performance by roughly 3%. Replacing the kernel 2 × 2 by 3 × 3 would also result in a drop roughly 2% in performance. Either substituting the max pooling type for average pooling type or substituting the tang activation function for ReLU activation function reduces the performance by roughly 1%. Using the Stochastic Gradient degree resulted in a drop nearly 8%.

(2) Performance comparison with DenseNet

For DenseNet, the size of input image is 224 × 224 and adopt 11 × 11 or 5 × 5 kernels in the first few layers. We change the DenseNet kernel as 3 × 3 in order to compare our proposed method.

Table 4 Comparison of SK-DenseNet with DenseNet

	Kernel size	Number of Dense block	Activation function	Optimizer	Testing result (F_{avg})
DenseNet	3 × 3	[6,12,24,16]	Relu	Adam	0.933
SK-DenseNet	2 × 2	[6,12]	Relu	Adam	0.984

Table 5 The comparison of SK-DenseNet to other CNNs

Method	Testing result (F_{avg})
AlexNet	0.944
VGGNet	0.933
ResNet	0.962
Our proposed SK-DenseNet	0.984

Our proposed SK-DenseNet improves roughly 5% for ILD classification compared with DenseNet from Table 4.

(3) Performance comparison with other CNNs

Table 5 demonstrates a comparison of the proposed method with other CNNs, like AlexNet [19], VGGNet [20], and ResNet [12]. All methods of other CNNs were implemented by the originally proposed. The rest networks were designed for the color images classification of size 224 × 224. So, in order to fit the size, we rescaled the 32 × 32 lung patches to 224 × 224 and generated 3 channels according to that introduce in paper [5]. The results of our method outperformed 2%~4% than the rest of others. There are several reasons for other CNNs that performed poorly on the ILD classification: (i) They only use the previous layers' feature. They do not make full use of the features of all the previous layers of the neural network; (ii) the features in their ILD classifications are small, with the big kernel size that cannot capture small number of features in ILD.

5 Conclusion

In this paper, we presented an improved Dense-Net called small kernel DenseNet (SK-DenseNet) to classify lung HRCT image patches into 5 classes, healthy tissue, emphysema, ground glass, fibrosis, and micronodules. The architecture of proposed SK-DenseNet contains 2 dense blocks and 2 transition layers. Each dense block contains 6 groups. According to the characteristics of CT features of lung disease, the SK-DenseNet network is more effective to extract high level and small pathological features for ILD classification using a 2 × 2 convolution kernel. Experiment results show that the SK-DenseNet outperforms other CNNs, such as DenseNet, AlexNet, VGGNet, ResNet. In future, our study will focus on the annotated images with the ILD patter classification.

Acknowledgements This work is supported by the Natural Science Foundation of Zhejiang Province China, under Grant No. LY14F020036.

References

1. Abubakar II, Tillmann T, Banerjee A (2015) Global, regional, and national age-sex specific all-cause and cause-specific mortality for 240 causes of death, 1990-2013: a systematic analysis for the global burden of disease study 2013[J]. Lancet 385(9963):117–171

2. American Thoracic Society, European Respiratory Society (2002) American Thoracic Society/European Respiratory Society international multidisciplinary consensus classification of the idiopathic interstitial pneumonias [J]. Am J Respir Crit Care Med 165(2):277–304
3. Anthimopoulos M, Christodoulidis S, Christe A et al (2014) Classification of interstitial lung disease patterns using local DCT features and random forest [C]. Engineering in Medicine and Biology Society (EMBC), 2014 36th annual international conference of the IEEE. IEEE, pp 6040–6043
4. Anthimopoulos M, Christodoulidis S, Christe A et al (2014) Classification of interstitial lung disease patterns using local DCT features and random forest [C]. 36th annual international conference of the IEEE Engineering in Medicine and Biology Society (EMBC). IEEE, pp 6040–6043
5. Anthimopoulos M, Christodoulidis S, Ebner L et al (2016) Lung pattern classification for interstitial lung diseases using a deep convolutional neural network [J]. IEEE Trans Med Imaging 35(5):1207–1216
6. Carrington CB (1976) Interstitial lung disease (The 18th Aspen Lung Conference). Conference summary [J]. Chest 69(2 Suppl):322–328
7. Depeursinge A, Racoceanu D, Iavindrasana J et al (2010) Fusing visual and clinical information for lung tissue classification in high-resolution computed tomography [J]. Artif Intell Med 50(1):13–21
8. Depeursinge A, Vargas A, Platon A et al (2012) Building a reference multimedia database for interstitial lung diseases [J]. Comput Med Imaging Graph 36(3):227–238
9. Depeursinge A, Van de Ville D, Platon A et al (2012) Near-affine-invariant texture learning for lung tissue analysis using isotropic wavelet frames [J]. IEEE Trans Inf Technol Biomed 16(4):665–675
10. Gao M, Bagci U, Lu L et al (2018) Holistic classification of CT attenuation patterns for interstitial lung diseases via deep convolutional neural networks [J]. Comput Methods Biomech Biomed Eng Imaging Vis 6(1):1–6
11. Hahnloser RHR, Sarpeshkar R, Mahowald MA et al (2000) Digital selection and analogue amplification coexist in a cortex-inspired silicon circuit [J]. Nature 405(6789):947
12. He K, Zhang X, Ren S, et al (2016) Deep residual learning for image recognition[C]. In: 29th IEEE conference on computer vision and pattern recognition, CVPR 2016, IEEE Computer Society, pp. 770–778
13. Hinton GE, Osindero S, Teh YW (2006) A fast learning algorithm for deep belief nets [J]. Neural Comput 18(7):1527–1554
14. Hinton G, Deng L, Yu D et al (2012) Deep neural networks for acoustic modeling in speech recognition: the shared views of four research groups [J]. IEEE Signal Process Mag 29(6):82–97
15. Hoo-Chang S, Roth HR, Gao M et al (2016) Deep convolutional neural networks for computer-aided detection: CNN architectures, dataset characteristics and transfer learning [J]. IEEE Trans Med Imaging 35(5):1285
16. Huang G, Liu Z, Weinberger KQ et al (2017) Densely connected convolutional networks [C]. Proc IEEE Conf Comput Vis Pattern Recognit 1(2):3
17. Jacobs C, Sánchez C I, Saur S C, et al (2011) Computer-aided detection of ground glass nodules in thoracic CT images using shape, intensity and context features[C]. In: 14th international conference on medical image computing and computer assisted intervention, MICCAI 2011. Springer, Berlin, pp. 207–214
18. King TE Jr (2005) Clinical advances in the diagnosis and therapy of the interstitial lung diseases [J]. Am J Respir Crit Care Med 172(3):268–279
19. Krizhevsky A, Sutskever I, Hinton GE (2012) Imagenet classification with deep convolutional neural networks[C]. In: 26th annual conference on neural information processing systems, NIPS 2012, Neural information processing systems foundation, pp. 1097–1105
20. Simonyan K, Zisserman A (2014) Very deep convolutional networks for large-scale image recognition [J]. arXiv preprint arXiv:1409.1556
21. Song Y, Cai W, Zhou Y et al (2013) Feature-based image patch approximation for lung tissue classification [J]. IEEE Trans Med Imaging 32(4):797–808
22. Song Y, Cai W, Huang H et al (2015) Locality-constrained subcluster representation ensemble for lung image classification [J]. Med Image Anal 22(1):102–113
23. Sorensen L, Shaker SB, De Bruijne M (2010) Quantitative analysis of pulmonary emphysema using local binary patterns [J]. IEEE Trans Med Imaging 29(2):559–569
24. Uppaluri R, Hoffman EA, Sonka M et al (1999) Computer recognition of regional lung disease patterns [J]. Am J Respir Crit Care Med 160(2):648–654
25. Vos T, Barber RM, Bell B et al (2015) Global, regional, and national incidence, prevalence, and years lived with disability for 301 acute and chronic diseases and injuries in 188 countries, 1990–2013: a systematic analysis for the global burden of disease study 2013[J]. Lancet 386(9995):743–800
26. Wang Y, Lin X, Wu L et al (2017) Effective multi-query expansions: collaborative deep networks for robust landmark retrieval [J]. IEEE Trans Image Process 26(3):1393–1404
27. Wang Y, Wu L, Lin X, Gao J (2018) Multiview spectral clustering via structured low-rank matrix factorization. In: IEEE transactions on neural networks and learning systems, p. 99
28. Wu L, Wang Y, Li X et al (2018) Deep attention-based spatially recursive networks for fine-grained visual recognition [J]. IEEE Trans Cybern PP(99):1–12

29. Wu L, Wang Y, Gao J, Li X (2018) Deep adaptive feature embedding with local sample distributions for person re-identification. Pattern Recogn 73:275–288
30. Wu L, Wang Y, Li X, Gao J (2018) What-and-where to match: deep spatially multiplicative integration networks for person re-identification. Pattern Recogn 76:727–738
31. Xu Y, Sonka M, McLennan G et al (2006) MDCT-based 3-D texture classification of emphysema and early smoking related lung pathologies [J]. IEEE Trans Med Imaging 25(4):464–475
32. Zhang S, Zhao X (2013) Dimensionality reduction-based spoken emotion recognition [J]. Multimed Tools Appl 63(3):615–646
33. Zhao X, Zhang S (2011) Facial expression recognition based on local binary patterns and kernel discriminant isomap [J]. Sensors 11(10):9573–9588
34. Zhao X, Shi X, Zhang S (2015) Facial expression recognition via deep learning [J]. IETE Tech Rev 32(5):347–355

Wenping Guo He received his MSc in computer science from Southwest Jiaotong University, China, in 2005. He was a visiting scholar at Jacksonville State University, USA, from February 2012 to June 2012. He is currently an associate professor at Taizhou University, China and a PhD candidate in computer science at Hohai University, China, with research interests including deep learning and health data analytics.

Zhuoming Xu He received his BSc and MSc in computer science from Hohai University, China, in 1986 and 1994 respectively, and his PhD in computer science from Southeast University, China, in 2005. He was a visiting professor at Indiana University Bloomington, USA, from May 2011 to May 2012. He is currently a full professor in College of Computer and Information at Hohai University, China. His current research interests include Web data management and multimedia annotation.

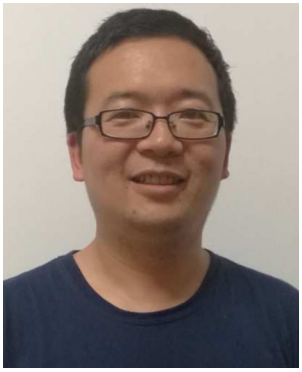

Haibo Zhang He received his BSc in environmental sciences from Qingdao University of Technology, China in 2004 and MSc in computer science from China University of Petroleum, China, in 2008. He is currently an experimentalist at Taizhou University, China with research interests including machine learning and E-health data mining.